ISOTOPIC ARCHIVES OF SULPHATE IN SPELEOTHEMS

Peter M. Wynn[a]*, Ian. J. Fairchild[b], Andy Baker[b], James U.L. Baldini[c], Frank McDermott[d]

[a] *Department of Geography, University of Lancaster, Lancaster, LA1 4YQ, UK*

[b] *School of Geography, Earth and Environmental Sciences, University of Birmingham, Birmingham, Edgbaston, B15 2TT, UK*

[c] *Department of Earth Sciences, University of Durham, Durham, DH1 3LE, UK*

[d] *School of Geological Sciences, University College, Dublin, Belfield, D4, Ireland*

* Corresponding author. Tel. +44(0)1524 510235. E-mail address: p.wynn@lancaster.ac.uk

ABSTRACT

The hemispheric impact of industrial emissions upon atmospheric sulphur loading is reflected in the sulphur depositional history recorded in cores from ice sheets. However, these do not reveal regional variations. Recently deposited speleothems are used here as archives of regional sulphur depositional history at two locations within the United Kingdom and Ireland. $\delta^{34}S\text{-}_{SO_4}$ and $\delta^{18}O\text{-}_{SO_4}$ present within speleothem carbonate are measured for the first time as part of a dual isotope approach to decode the speleothem sulphur record. The largely refractory nature of $\delta^{34}S\text{-}_{SO_4}$ under oxidising conditions enables source provenance of atmospheric SO_2, whereas the complex cycles of isotopic exchange and fractionation during incorporation of oxygen into sulphate molecules enable $\delta^{18}O\text{-}_{SO_4}$ signatures to yield insights into ambient environmental conditions and biogeochemical cycling in the ecosystem above the cave. $\delta^{34}S\text{-}_{SO_4}$ values extracted from speleothem carbonate formed within Browns Folly Mine, UK, range from +3.5 to +5.5 ‰ and $\delta^{18}O\text{-}_{SO_4}$ +10.3 to +13.7 ‰. Both signatures lie within the range expected from sulphate deposition in industrial locations and reflect the transfer of sulphate into speleothem calcite with little fractionation. However, $\delta^{18}O\text{-}_{SO_4}$ signatures at Crag Cave, western Ireland, are isotopically heavier than expected and approach isotopic equilibrium with $\delta^{18}O\text{-}_{H_2O}$ under reducing conditions. Dual isotope analysis of $\delta^{34}S\text{-}_{SO_4}$ and $\delta^{18}O\text{-}_{SO_4}$ optimises the correct identification of sulphur sources and biogeochemical cycling prior to incorporation into the speleothem record. At carefully selected cave sites where drip water flowpaths into the cave remain oxic, speleothems hold the potential to retain records of atmospheric sulphur loading at the local and regional scale.

Keywords: Sulphur isotopes, Sulphate-oxygen isotopes, speleothems, atmospheric sulphur

1. INTRODUCTION

Anthropogenic emissions of SO_2 have risen since 1850 due to increased industrial activity (LeFohn et al., 1999), rendering atmospheric sulphate aerosols key agents in forcing recent climate (e.g. Smith et al., 2001). Such increased emissions are documented in ice core records of sulphate deposition, which are currently considered the premier archive of past atmospheric sulphur concentrations (e.g., Patris et al., 2000, 2002; Isaakson et al., 2005). However, ice core localities are frequently distal from sources of SO_2 emissions and reflect a relatively clean atmospheric boundary layer. Due to the relatively short lifetime of sulphate aerosols in the atmosphere, the impact of anthropogenic sulphur emissions on the climate and biogeochemistry of sulphur cycling is most acute at local and regional scales. Historical quantification of sulphur inputs to terrestrial environments has been demonstrated through sulphur isotope ratios in archived soil and herbage samples from the UK (Zhao et al., 1998), from wood of coniferous trees in Japan (Kawamura et al., 2006) and from lake and peat sediment cores in Europe (Bottrell and Coulson, 2003; Coulson et al., 2005; Novak et al., 2005) and Canada (Mayer et al., 2007).

Speleothems can yield multi-proxy, high resolution records of the palaeoenvironment, and are formed through the carbonation of host carbonate bedrocks and re-precipitation of calcite within cave environments (see review by Fairchild et al., 2006a). The incorporation of trace elements, organic molecules and specific stable isotope signatures in speleothem carbonate provides a suite of geochemical parameters capable of capturing a cave's response to the external environment. Thus, trace amounts of sulphur discovered as sulphate in speleothems suggest that stalagmites may record key aspects of atmospheric variability in sulphate content at local and regional scales (Frisia et al., 2005; Fairchild et al., 2006a). Sulphate is

inferred to be present in speleothem calcite as Carbonate Associated Sulphate (CAS) identified in the geological record of marine carbonates (e.g. Bottrell and Newton, 2006). XANES analysis has been used in both marine (Pingitore et al., 1995) and speleothem carbonate (Frisia et al., 2005) to identify the oxidation state of the constituent sulphur as sulphate, implying its presence within the calcite lattice as a structural substitution for carbonate. However, sulphur concentration data alone cannot directly identify the source of speleothem CAS (Wadleigh et al., 1996; Frisia et al., 2005). Atmospheric variability in sulphate content is controlled by natural as well as anthropogenic sources of sulphur and may be modified by biogeochemical cycling and additional sources of sulphur stored within the surrounding bedrock and soil waters (Figure 1). The sulphate content of cave drip waters and associated stalagmites may thus represent a mixed signal, reflecting not only the local variability in atmospheric sulphate content, but also biogeochemical cycling in the ecosystem above the cave. Sulphur and oxygen isotope systematics of sulphate differ markedly, and in principle should enable the provenance of sulphate within speleothems to be established permitting further deconvolution of the mixed atmospheric / biogeochemical signal archived within speleothems.

2. THEORETICAL BACKGROUND

Figure 1 summarises the potential sources of sulphate contributing to speleothem CAS with characteristic $\delta^{34}S$ compositions. Primary sea-salt aerosols released into the atmosphere from sea spray are derived from the well-mixed reservoir of marine sulphate and have a $\delta^{34}S$ value identical to that of sea water (~ +21 ‰). Biogenic sources of secondary sulphate aerosol are derived from marine emissions of

dimethylsulphide (DMS) and are generally depleted in ^{34}S relative to seawater sulphate, with reported $\delta^{34}S$ values of +15.6 ±3.1 ‰ (Calhoun et al., 1991). Continental emissions of sulphate aerosol can be divided into anthropogenic and biogenic emissions. In the northern hemisphere, sulphate in precipitation sourced predominantly from anthropogenic emissions is usually assigned an average $\delta^{34}S$ value between -3 and +9 ‰ (Mayer, 1998), despite the $\delta^{34}S$ composition of the source materials varying beyond this range (see compilation of source material values in Nielson, 1974). Continental biogenic emissions of sulphur consist predominantly of gaseous organic sulphides from the decomposition of organic matter associated with plants and soils. Such emissions have a wide range of $\delta^{34}S$ values depending upon the redox status under which they are formed. Under oxidising conditions, their isotopic composition should be similar to that of local precursor sulphate derived from precipitation, groundwater and lithogenic sources. This is quoted to have an average $\delta^{34}S$ value close to 0 ‰ (Nielson, 1974), although reducing conditions induce extensive fractionation to the source compounds. This fractionation varies with environmental conditions although when the size of the substrate pool is unlimited, gaseous organic sulphides may be fractionated so they are up to 70 ‰ lighter than the precursor sulphate (Brunner and Bernasconi, 2005).

Due to the widely differing source composition of oxygen isotopes involved in the oxidation of sulphur compounds to sulphate, the oxygen isotopic composition of sulphate in speleothems should enable the distinction between sulphate which is sourced directly from the atmosphere and that produced by nutrient cycling in terrestrial ecosystems (e.g.: Mayer et al., 1995a, b; Likens et al., 2002), thus aiding process- identification as well as source provenance. Published values for the $\delta^{18}O$

composition of atmospheric sulphate range from -3 to +41.7 ‰ V_{SMOW} (see compilation of published values in Jamieson and Wadleigh, 1999; Jenkins and Bao, 2006). This wide range reflects the different reaction pathways of gaseous sulphide oxidation in the atmosphere, the oxygen isotopic composition of the oxidants involved and the mixing ratio between aerosols formed at source as sulphate (primary aerosols) and those produced in the atmosphere from gaseous precursors (secondary aerosols) (see review by Holt and Kumar, 1991). Secondary aerosols formed from gaseous precursors do not carry oxygen isotopic signatures indicative of source provenance, but reflect only the pathways of sulphide oxidation in the atmosphere due to a rapid isotopic equilibration between reduced sulphoxy intermediate species and H_2O. Source provenance signatures of $\delta^{18}O$ in reduced sulphur compounds emitted into the atmosphere are thus erased during oxidation to secondary aerosol species. Primary sulphate aerosols retain their source $\delta^{18}O\text{-}_{SO_4}$ composition during transport through the atmosphere. These can be sourced from sea spray (+9.7 ‰; Lloyd, 1967) or from industrial activity with $\delta^{18}O\text{-}_{SO_4}$ signatures up to +45 ‰ (Holt et al., 1982; Jamieson and Wadleigh 1999). The proportion of primary aerosol present in the atmosphere thus significantly influences the value of bulk $\delta^{18}O\text{-}_{SO_4}$ aerosol deposition.

Subsequent to sulphate aerosol deposition, biogeochemical cycling of sulphur resets the oxygen isotopic composition of atmospheric-derived sulphate according to environmental conditions. Where aerobic oxidising conditions prevail in the overlying cave soils, biogeochemical cycling of deposited sulphate may induce assimilatory sulphate reduction to organic-S compounds and mineralisation back into the inorganic phase. This causes only minimal fractionation to $^{34}S/^{32}S$ ratios compared to precursor sulphate derived from precipitation, groundwater and lithogenic sources. Sulphate

$^{18}O/^{16}O$ ratios however, are a product of incorporating four oxygen atoms obtained in varying proportions from the surrounding soil water and atmospheric oxygen (Equation 1).

$$\delta^{18}O\text{-}_{SO_4} = [(\delta^{18}O_{atm\ O_2} - \varepsilon_{SO_4\text{-}atm}) \times f_{O2\ atm}] + (\delta^{18}O_{water} \times 1\text{-}f_{O_2\ atm}) \quad (1)$$

where $f_{O_2\ atm}$ and $1\text{-}f_{O_2\ atm}$ represent the fraction of oxygen obtained from the atmosphere and soil water respectively, and $\delta^{18}O\text{-}_{atm\ O_2}$ and $\delta^{18}O\text{-}_{water}$ represent the oxygen isotopic compositions of atmospheric O_2 (+23.88 ‰; Barkan and Lus, 2005) and water. $\varepsilon_{SO_4\text{-}atm}$ is the isotopic enrichment associated with the incorporation of atmospheric O_2 into sulphate, demonstrated experimentally to have a value of -8.7 ‰ (Lloyd, 1968).

Sulphoxy intermediate compounds (SO, SO_2, HSO_3^-) can be exposed to rapid isotopic equilibration with the surrounding water. The isotopic composition of the constituent oxygen can thus be reset such that up to 75% of the oxygen in the final sulphate molecule has an isotopic composition controlled by meteoric water (Holt, 1981). Where mineralisation of organic compounds to sulphate is sufficiently rapid such that sulphoxy intermediate species do not become fully equilibrated with meteoric water, the final sulphate molecule may contain a greater proportion of oxygen sourced from atmospheric O_2 (Bottrell, 2007). The $\delta^{18}O\text{-}_{CAS}$ contained within speleothem calcite is thus sensitive to the relative proportions of atmospheric O_2 and water oxygen incorporated into the sulphate molecule. Isotopic signatures may therefore have a theoretical upper end-member composition of +14.8 ‰ where all four oxygen atoms are derived from atmospheric O_2 (Bottrell and Newton, 2006) and range towards the

oxygen isotopic composition of the ambient water where equilibration with meteoric water imparts up to 75% of the isotopic composition. Where sulphur is contained within organic matter as ester sulphate compounds and liberated through enzyme hydrolysis (e.g. Fitzgerald, 1976), at least three of the oxygen atoms in the newly mineralised sulphate are sourced directly from the organically bound sulphate molecule. As such, a depletion of only 2-3 ‰ is observed in oxygen isotope composition compared to the original sulphate ester compound (Mayer et al., 1995b).

Under reducing conditions, processes of microbial sulphate reduction may cause extensive kinetic fractionation of $\delta^{34}S$. Fractionation of $\delta^{18}O\text{-}_{SO_4}$ however, is manifest as an equilibrium isotopic exchange between the ambient water and the residual sulphate pool such that an enrichment factor of +29 ‰ at 5 °C may be apparent if equilibrium is approached (Fritz et al., 1989; Brunner et al., 2005; Wortmann et al., 2007). During initial stages of sulphate reduction, $\delta^{34}S\text{-}_{SO_4}$ and $\delta^{18}O\text{-}_{SO_4}$ signatures demonstrate a linear fractionation relationship, typical of a kinetic reaction mechanism. When sulphate reduction reaches an advanced state however, residual $\delta^{18}O\text{-}_{SO_4}$ signatures approach a constant equilibrium value and $\delta^{34}S\text{-}_{SO_4}$ residual signatures continue to become enriched in ^{34}S according to a typical Rayleigh fractionation trajectory (Brunner et al., 2005). Where cyclical reduction - re-oxidation of sulphate occurs within the same environment, values of $\delta^{18}O\text{-}_{SO_4}$ may display an offset between the equilibrium oxygen isotope signature and the measured values. Re-oxidation of sulphite to sulphate involves the incorporation of one additional oxygen from an external source such as water (enrichment factor = + 4 ‰; cf.Taylor et al., 1984). The resulting oxygen isotope composition in the residual sulphate can be approximated as;

$$\delta^{18}O\text{-}_{SO_4} = [0.75 \times (\delta^{18}O_{H_2O} + \varepsilon_{SO_4\text{-}H_2O})] + 0.25 \times (\delta^{18}O_{H_2O} + 4\ ‰)] \quad (2)$$

where $\varepsilon_{SO_4\text{-}H_2O}$ is the equilibrium isotopic enrichment between $\delta^{18}O$ in the residual sulphate pool and that in the surrounding water (after Brunner et al., 2005). The influence of re-oxidation upon ^{34}S values however will be to retain a signature similar to the initial products if isotope mass balance is maintained (e.g., Barker et al., 1998). The extraction and analysis of $\delta^{34}S$ and $\delta^{18}O$ from speleothem CAS thus holds the potential to record the sulphur sources and biogeochemical transformations present along the flow pathways of speleothem-feeding drips.

Traditional methods used for the extraction and analysis of SO_4-S and SO_4-O from carbonates rely on the acid digestion of large quantities of material (typically 100 to 300 g) and the extraction of sulphate as barium sulphate (e.g. Gellatly and Lyons, 2005). The large volumes of carbonate material required have thus frequently constrained the type of samples analysed for sulphate isotopic composition. Where geological carbonates are present in abundance or contain significant quantities of sulphur, such constraints are not applicable. However, in speleothem carbonate, sulphur content is low and the material available for analysis is necessarily limited. New methods to reduce the sample size of carbonate material required for the extraction and analysis of $\delta^{34}S\text{-}_{SO_4}$ and $\delta^{18}O\text{-}_{SO_4}$ have been developed as a part of this study, thus enabling the sulphur isotopic characterisation of speleothem archives. Here we report the first determinations of $^{34}S/^{32}S$ and $^{18}O/^{16}O$ ratios of CAS extracted from speleothems. The samples originate from two cave sites in contrasting locations, demonstrating the power of the dual isotope approach for palaeoenvironmental

interpretation. We compare modern time series of a stalagmite collected from within Browns Folly Mine, UK, where values of δ^{34}S-$_{CAS}$ illustrate a dominant control by anthropogenic SO_2 emissions, with that of a stalagmite from Crag Cave, S.W Ireland, yielding δ^{34}S-$_{CAS}$ and δ^{18}O-$_{CAS}$ signatures representative of sulphate reduction and re-oxidation in the soils above the cave.

3. SITE AND SAMPLE DESCRIPTION

Browns Folly Mine, Bathford, SW England, was developed in the 19th century for the extraction of building stone from the surrounding limestone (the Bath Oolite member of the Jurassic Great Oolite series) (for cross section of mine site see Baldini et al., 2005; Fairchild et al., 2006b). Mining activity commenced in 1836 and continued until the mines were abandoned in 1886, thus constraining the maximum possible age of the associated speleothems. The mines remained closed for approximately 100 years until re-opened by cavers in the 1970s (Baker et al., 1998, 1999). Lithologies of the overlying Middle Jurassic bedrock are mainly oolitic and skeletal limestones, containing a minor sand and clay component and a porosity of 0 to 40 % (Fairchild et al., 2006b), with an absence of pyrite and other sulphide minerals. Vertical fractures dissect the horizontally stratified limestone formations providing a route for rapid fissure flow of groundwater into the mine system. Slower seepage flow is fed by minor fissures and water stored within the porous limestone matrix (Baker et al., 1999; Fairchild et al., 2006b). Vegetation has gradually re-established itself over the study site since the cessation of mining operations in 1886 such that secondary deciduous forest of mixed ash, sycamore and oak is now prevalent (Baldini et al., 2005). The sampled stalagmite (BFM-Boss) was extracted in 1996 from a chamber

276 approximately 300 m from the mine entrance (Baldini et al., 2005) and represents a
277 continuous deposition of calcite in annual couplets of clear and inclusion-rich
278 laminae. Three independent lamina thickness counts established 77±3 annual couplets
279 at the central growth axis suggesting that BFM-Boss nucleated no later than 1916.
280 Annual calcite deposition rates remained low until 1975, when couplet thicknesses
281 increase dramatically, indicating an increase in growth rate. The nucleation of BFM-
282 Boss approximately 30 years after the closure of the mines is thought to reflect either
283 the time taken for the development of a stable hydrological system subsequent to the
284 cessation of mining activity, or the slow rate of vegetation establishment above the
285 cave site. Baldini et al., (2005) showed that vegetation development had a strong
286 influence on the $\delta^{13}C$ and $\delta^{18}O$ record of this sample.
287
288 Crag Cave, located in County Kerry, Ireland, is developed in Lower Carboniferous
289 limestone some 20 km from the Atlantic coast of SW Ireland (McDermott et al.,
290 1999) (for site details see Tooth and Fairchild 2003; Baldini et al., 2006). Discovered
291 in 1981, parts of the relatively shallow cave system (c. 20m deep) were opened as a
292 tourist cave in 1985, although restricted access to the cave interior has ensured the
293 maintenance of near-pristine conditions, rendering it ideal for hydrochemical studies
294 (Baldini et al., 2006). The surrounding bedrock, belonging to the Lower
295 Carboniferous Cloonagh Formation is dominantly limestone, with small amounts of
296 dolomite and some pyrite (Tooth and Fairchild, 2003). Till deposits overlying the
297 cave are of variable thickness (0.1-2.5m thickness) belonging to the Munsterian
298 (Marine Isotope Stage 6) glaciation. The low permeability of the fine grained clay
299 matrix encourages saturation and a constant supply of water to the stalagmite-feeding
300 drips, and streaks of iron oxide staining demonstrate the presence of oxidising

conditions in isolated zones and hence the existence of redox cycling. The presence of a crack and fissure network allows the till deposits to be regarded as a dual-porosity system, facilitating both rapid water throughput via fracture flow and a more constant matrix seepage flow supplied from the large storage capacity of the micropores (Tooth and Fairchild, 2003). The sampled stalagmite, CC-Bil, was removed from a passage 30 m below the ground surface in 2002. The drip that fed stalagmite CC-Bil formed on the tip of a 1m long soda straw stalactite and is classed as a 'seepage flow site' under the classification of Smart and Friederich (1986). Drip rates at this site and others in close proximity are low (site CC-Bil = 0.08 ml/min) and show very little variation through time (site CC-Bil drip rate CV = 5.4 %) (Tooth and Fairchild, 2003; Baldini et al., 2006). Based on visible calcite deposition on loggers underneath the drip feeding stalagmite CC-Bil, this stalagmite was actively growing when collected in 2002. U-series dating demonstrates a basal mean ICP-MS U-Th age of 1752 AD (+/- 7 years) and an approximately linear growth rate over the past 260 years.

4. METHODOLOGY

4.1. Sulphate extraction

Sulphur concentrations in each of the stalagmites were determined by high resolution inductively coupled plasma mass spectrometric analysis (HR-ICPMS) of calcite powders at Kingston University, UK, drilled in 2 mg aliquots from the central axis of the stalagmite and digested in 8 ml of 2 % HNO_3 (Aristar grade). Depending upon the concentration of CAS, larger aliquots of calcite (~200 mg) were prepared for sulphur and oxygen isotope analysis by sampling in a continuous fashion down the stalagmite central growth axis, each sample aggregating several years of growth. Using the concentration data obtained through HR-ICPMS analysis, the size of each carbonate sample was calculated to yield a minimum of 35 μg of sulphur, representing the quantity of sulphur required for analysis by CF-IRMS (continuous flow isotope ratio mass spectrometry) given the instrumental

328 configuration outlined below. Parallel sampling tracks enabled the integrity of $\delta^{34}S$ and $\delta^{18}O$ analyses
329 to be assessed through sample replication. The methodological approach to sulphur and oxygen isotope
330 extraction was based upon procedures reported in Newton et al. (2004), albeit simplified as the relative
331 purity of stalagmite carbonate precluded the need for pre-treatment with sodium hypochlorite and
332 bromine water to remove organic contaminants and trace amounts of pyrite, respectively. Given the
333 small quantities of sulphur extracted per sample, the following protocol was designed to minimise
334 sample handling and contamination in all steps of the procedure.
335
336 Drilled stalagmite powders were digested overnight in 1 ml of 4M hydrochloric acid (Aristar grade)
337 within polyethylene syringes, capped with Luer tips. Syringe filtration through pre-rinsed 0.2µm nylon
338 filter capsules (Puradisc, Whatman®) enabled sample transfer between vessels with the minimum of
339 product loss. The extraction of sulphate as barium sulphate was undertaken following precipitation
340 using barium chloride solution. Two different techniques of precipitate concentration were used to
341 collect the barium sulphate from solution: filtration and centrifugation. Where filtration was the method
342 employed, 0.5 ml of 1 M barium chloride solution was added to the filtered carbonate digest solution
343 within the housing of a second polyethylene syringe. Samples were left to precipitate and mature for 2
344 – 3 days, prior to syringe filtration through quartz microfibre filters using an in-line filter capsule
345 (Swinnex, millipore) modified to hold filter papers 7 mm in diameter. Each filter loaded with 35 µg of
346 S (~250 µg $BaSO_4$) was transferred into a tin capsule, dried at 70 °C and stored in a desiccator prior to
347 mass spectrometric analysis (Figure 2).
348
349 However, based upon the decomposition of quartz above 700 °C and the release of constituent oxygen,
350 the use of quartz microfibre filters as a means of pre-concentrating barium sulphate precluded analysis
351 for $\delta^{18}O\text{-}SO_4$ by this method. Centrifugation in association with an inert medium was thus employed as
352 the method of pre-concentration for the remainder of the study. Carbonate digest solutions were
353 syringe-filtered into 1.5 ml centrifuge vials and precipitated as barium sulphate following addition of
354 0.2 ml of 1M barium chloride solution. Contact time between free sulphate ions in solution with strong
355 acid was minimised to ~ 1 hour to prevent potential oxygen isotopic exchange between sulphate and
356 water under acidic conditions (e.g. Gellatly and Lyons, 2005; Newton et al., 2004; Hurtgen et al.,
357 2002). Addition of quartz powder (~ 2 mg; EuroVector isotopic grade) served as an inert medium onto

which barium sulphate could precipitate, thus increasing the mass of product and enabling ease of handling. Sulphate for $\delta^{18}O$ analysis was precipitated onto powdered glassy carbon (~ 0.5 mg, Euro Vector isotopic grade) as the inert medium. Samples of barium sulphate were left to mature for ~72 hours prior to repeated centrifuging and washing with de-ionised water to remove excess barium. The resultant pellets of quartz powder with barium sulphate and glassy carbon with barium sulphate were oven dried at 70 °C and transferred to tin or silver capsules for $\delta^{34}S$ and $\delta^{18}O$ analysis respectively (Figure 2).

To overcome possible problems associated with oxygen release during the decomposition of quartz powder contributing to SO_2 beam intensities and thus influencing $\delta^{34}S$ measurements (e.g. Fry et al., 2002), similar quantities of quartz powder were added to standard materials as well as samples prior to combustion. This effectively supplied a large reservoir of oxygen in the form of quartz powder, buffering the oxygen composition of the SO_2 gas for both samples and standards.

4.2. Mass spectrometric analysis

$^{34}S/^{32}S$ and $^{18}O/^{16}O$ ratios of product barium sulphate were determined using a EuroVector elemental analyser linked to a GV Isoprime continuous flow mass spectrometer at the University of Birmingham. Combustion of samples within tin capsules in the presence of vanadium pentoxide at 1030 °C yielded SO_2 for determination of $\delta^{34}S$-SO_4 and pyrolysis within silver capsules in the presence of nickelised carbon at 1250 °C yielded CO for determination of $\delta^{18}O$-SO_4. $\delta^{34}S$ values were corrected against CDT using within run analyses of international standard NBS-127 and SO5 (assuming $\delta^{34}S$ values of +20.3 ‰ and +0.5 ‰ respectively (IAEA, 2004)) and $\delta^{18}O$ was corrected to VSMOW using NBS-127 and SO6 (assuming $\delta^{18}O$ values of +9.3 ‰ and -11.3 ‰ respectively (IAEA, 2004)). Within-run standard replication (1 SD) was <0.3 ‰ for both sulphur and oxygen. Sample replication from two parallel sample tracks drilled in stalagmite BFM-Boss were < 0.4 ‰ (1 SD) for $\delta^{34}S$ values and < 0.5 ‰ for $\delta^{18}O$ values based on sample replication in stalagmite CC-Bil.

Procedural standard solutions of calcium sulphate and sodium sulphate were used to test the integrity of the methodology for precipitation and analysis of small quantities of barium sulphate for $\delta^{34}S$ and $\delta^{18}O$

388 determinations respectively. Calcium sulphate solution precipitated as barium sulphate under acidified
389 conditions and analysed according to the above methodology using quartz microfibre filters, yielded
390 $\delta^{34}S\text{-}SO_4$ signatures of +3.2 ‰ (0.3 ‰ 1 SD, n = 20) compared to $\delta^{34}S$ values of +2.9 ‰ (0.3 ‰ 1 SD,
391 n = 13) for analysis of raw calcium sulphate powder. Where centrifuging with quartz powder was used
392 as the method of pre-concentration, analyses of standard calcium sulphate solution precipitated as
393 barium sulphate, yielded $\delta^{34}S\text{-}SO_4$ isotopic values of +2.6 ‰ (0.3 ‰ 1 SD, n = 12). Sodium sulphate
394 solution precipitated as a bulk quantity of barium sulphate yielded $\delta^{18}O\text{-}SO_4$ isotopic signatures of +12.6
395 ‰ (0.4 ‰ 1 SD, n = 8) compared to analyses obtained following the centrifuging method of pre-
396 concentration under analogous acidified conditions, of +13.0 ‰ (0.7 ‰ 1 SD, n = 6).
397
398 Blank contamination associated with $\delta^{34}S$ determinations were zero. A small blank signal associated
399 with oxygen analysis is most likely associated with trace levels of oxides on the glassy carbon and
400 nickelised carbon catalyst, but was too small to determine accurately. To overcome the potential impact
401 of blank contribution upon reported $\delta^{18}O$ values, standard materials and samples were analysed using
402 the same quantities of glassy carbon powder and nickelised carbon catalyst.
403
404 ## 5. RESULTS
405
406 ### 5.1. BFM-Boss
407
408 Figure 3 displays sulphur concentrations and $\delta^{34}S$ and $\delta^{18}O$ values of carbonate
409 associated sulphate in stalagmite BFM-Boss. Sulphur concentrations are between 150
410 to 250 ppm (Table 1) and are coincidentally similar to those of the surrounding
411 bedrock (range 156 to 312 ppm) (Table 2). The $\delta^{34}S\text{-}CAS$ values associated with BFM-
412 Boss are between +3.5 and +5.5 ‰ and significantly lower than those contained
413 within the surrounding bedrock (+17.9 to +22.0 ‰). $\delta^{18}O\text{-}CAS$ signatures within the
414 speleothem range between +10.3 ‰ to +13.7 ‰. Table 3 displays the ionic
415 composition of the feeding drip-water to stalagmite BFM-Boss. Sulphate

concentrations displayed as a percentage sea-salt sulphate (% SSS) are calculated on the assumption that sea spray has a molar SO_4/Cl ratio of 0.0516 and is the source of all Cl^- in the drip waters (after Holland, 1978), such that 29 % (1 SD = 15%) of all sulphate is calculated to be of inorganic marine provenance. Further, sulphate concentrations within drip waters comprise just 1.4 % sulphate sourced from the bedrock based on Ca/SO_4 ratios given in Table 2 (equation 3).

$$^{\%\ bedrock}SO_4 = [1 / (^{bedrock}\ Ca{:}SO_4 / {}^{dripwater}Ca) / {}^{dripwater}\ SO_4] \times 100 \quad (3)$$

This assumes all calcium in the cave drip waters is sourced from dissolution of the karst bedrock, with negligible contribution from dissolution of calcareous dust particulates in the atmosphere, and assumes ratios are unaffected through chemical evolution associated with limited levels of prior calcite precipitation (Tooth and Fairchild, 2003).

5.2. CC-Bil

Sulphur concentrations within stalagmite CC-Bil are between 100 and 200 ppm and values of $\delta^{34}S\text{-}_{CAS}$ range between +16.8 and +19.1 ‰ and $\delta^{18}O\text{-}_{CAS}$ between +19.2 and +23.9 ‰ (Table 4, Fig 4). Bedrock concentrations of sulphur are low and range between 51 and 92 ppm (Table 2), and isotopes of $\delta^{34}S$ and $\delta^{18}O$ within the lower Carboniferous limestone within which Crag Cave is formed are reported to range between +13 to +15 ‰ for $\delta^{34}S$ based on CAS-derived S isotopes and +14 to +19 ‰ for $\delta^{18}O$ based on marine evaporites (Bottrell and Newton, 2006). Drip sites feeding and immediately adjacent to stalagmite CC-Bil display sulphate concentrations which

441 are consistently between 7.9 to 8.5 ppm. % SSS consistently accounts for 36 % of the
442 measured drip water sulphate and % bedrock-derived sulphate represents just 1.1 % of
443 drip water sulphate composition (Table 4).
444
445 **6. DISCUSSION**
446
447 **6.1. Browns Folly Mine; BFM-Boss**
448
449 On the understanding that the chloride content of cave drip waters can be used as an
450 indicator of primary sea spray aerosol content at each site, apportionment of
451 speleothem CAS between the remaining sources is possible using the $\delta^{34}S$ end
452 member compositions and $\delta^{18}O$ process information outlined above. Based on the
453 %SSS content and ratio of calcium to sulphate in cave drip waters feeding stalagmite
454 BFM-Boss (Table 3), 29 % of the constituent sulphate appears to be of primary
455 marine origin and just 1.4 % is sourced from the carbonate bedrock. As the $\delta^{34}S$
456 marine end-member value for primary sea salt aerosol is +21‰ and the bedrock has
457 an average $\delta^{34}S$ composition of +20 ‰, mass balance suggests the additional source
458 of sulphur contributing to contemporary speleothem CAS must have a $\delta^{34}S$ value
459 close to -3 ‰ (actual measured $\delta^{34}S$ composition +3.5 to +5.5 ‰). On the basis that
460 anthropogenic emissions of sulphur in precipitation are documented to reside between
461 -3 and +9 ‰ in industrialised countries of the northern hemisphere (Mayer, 1998),
462 this would suggest the non sea salt sulphur within stalagmite BFM BOSS is derived
463 predominantly from anthropogenic pollution (e.g., Zhao et al., 1998) (Fig. 5). Such an
464 interpretation is consistent with the industrial nature of the region surrounding this
465 particular site. Continental biogenic emissions of reduced sulphur compounds may

466 also have $\delta^{34}S$ values within the range required to account for the additional source of
467 sulphur contributing to speleothem CAS. However, oxidation of such biogenic
468 emissions within the atmosphere would render the constituent oxygen isotopes too
469 light to account for the source of speleothem sulphate (see Figure 5). Bedrock-derived
470 CAS $\delta^{34}S$ values (+17.8 to +21.9 ‰) are considerably higher than sulphate
471 structurally bound within stalagmite calcite. Release of this heavy bedrock sulphate
472 into groundwaters may contribute an additional source of sulphate to the drip water,
473 although in the most recently deposited speleothem calcite, bedrock sulphate
474 contributes just 1.4 % of the total stalagmite CAS composition. $\delta^{34}S$ values are stable
475 between 1960 to 1992 at ~ +3.6 ‰, although calcite deposited prior to 1962 hosts
476 $\delta^{34}S\text{-}_{CAS}$ values up to +5.5 ‰. This may reflect lower sulphur emissions from
477 industrial activity during the early 20th C and relatively greater contributions from
478 marine and bedrock derived sources with heavier sulphur isotopic composition. The
479 lack of co variation between sulphur concentrations and sulphur isotopes post 1960
480 may reflect the dominant source of anthropogenic sulphur in the atmosphere. The
481 minimal relative contribution from additional sulphur sources may cause little
482 perturbation from pollution end-member compositions.
483
484 $\delta^{18}O\text{-}_{CAS}$ signatures range from +10.3 ‰ to +13.7 ‰, with the heavier isotopic values
485 found during the earlier growth phases of the stalagmite. These signatures fall in a
486 range where interpretations of sulphur cycling in the sediments and biomass above the
487 cave are somewhat ambiguous. The $\delta^{18}O\text{-}_{CAS}$ compositions are similar to those
488 expected in atmospheric sulphate deposition (Figure 5) and could represent a direct
489 transfer of atmospheric precipitation into the cave environment via rapid flow routing,
490 having undergone very little biogeochemical transformation. Based on 29 % sea salt

sulphate contribution as primary marine aerosol ($\delta^{18}O\text{-}SO_4$ of primary marine aerosol is +9.7 ‰ (Lloyd, 1967)), the remaining non sea salt sulphate (NSS) in the youngest part of the stalagmite is calculated to have an end member composition of +10.9 ‰, typical for atmospheric sulphate deposition of mixed primary anthropgenic and secondary aerosol sulphate origin.

To produce drip water sulphate with $^{18}O/^{16}O$ ratios identical to those found in speleothem CAS via biogeochemical mineralisation of organic sulphur would require approximately 80 % of the constituent oxygen to be sourced from atmospheric O_2 (assuming fractionation during the mineralisation and incorporation of atmospheric oxygen into sulphate to be -8.7 ‰ (Lloyd, 1968) and an average drip water $\delta^{18}O\text{-}_{H_2O}$ composition of -5 ‰. However, given that experimental data have demonstrated biological reaction pathways may produce sulphate containing a maximum of 55 % atmospheric O_2 only under exceptional circumstances (Toran and Harris, 1989), the biogeochemical mineralisation of organic sulphur compounds to sulphate is not considered to be apparent in the drip water flow pathway feeding this stalagmite (Fig. 5).

If the main source of sulphate contained within organic matter is present as organic ester sulphate compounds, hydrolysis may produce free sulphate ions within a 2-3 ‰ range of the oxygen isotopic composition of the original sulphate compound (Mayer et al., 1995b). This would give an initial oxygen isotopic composition of approximately 12-13 ‰, consistent with an atmospheric aerosol source.

There is clear evidence at this cave site for both a long term hydrological storage component and a very rapid flow route at times of high rainfall (Fairchild et al., 2006b), thus both mechanisms (ester sulphate hydrolysis and rapid flow routing) remain possible contributors to the observed $\delta^{18}O$-CAS signatures at this site.

6.2. Crag Cave; CC-Bil

Crag Cave presents a contrasting case in being largely isolated from sources of anthropogenic SO_2 emissions and the large scale combustion of fossil fuels due to a predominantly westerly airflow and its position on the western periphery of Europe (Aherne and Farrell, 2002). Prevailing westerly winds typically provide the main source of atmospheric sulphur transporting aerosol of primary sea salt origin onto the continental margin (Aherne and Farrell, 2002; Jordan, 1997).

Ratios of sulphate to chloride in atmospheric deposition from the region typically define a sea salt component of ~80 % (Aherne and Farrell, 2002; Jordan, 1997), of which the remaining 20% could be sourced from DMS, distal sources of pollution, or continental biogenic emissions. This contrasts with ratios to chloride in drip waters feeding stalagmite CC-Bil, where just 35% of sulphate is of sea salt origin. This suggests an additional source of sulphur is obtained from somewhere along the drip water flow path. Values of $\delta^{34}S$-CAS in recent speleothem calcite are +18.6 ‰ (Table 4), leaving an end-member non sea salt sulphate composition of +17.2 ‰. This value appears typical of measured atmospheric deposition in the region (Bottrell and Novak, 1997; quoted average value of +17.8 ‰) although could represent any mixture of atmospheric sources stored within the soil profile as organic sulphur, prior to re-

mineralisation and release into the drip water flow path. Based on a comparison of Ca/SO_4 ratios in bedrocks and drip waters, carbonation and release of sulphate from the surrounding bedrock appears to contribute just 1.1 % of sulphate to the drip water composition and is thus insufficient to account for the additional sulphate source. Signatures of $\delta^{18}O\text{-}_{CAS}$ are used below to try and identify the nature of this additional non sea salt sulphate.

Values of $\delta^{18}O\text{-}_{CAS}$ are isotopically enriched in ^{18}O beyond that expected for values of atmospheric sulphate in an environment distal from extensive inputs of industrial pollution. $\delta^{18}O\text{-}_{CAS}$ values are also in excess of sulphate oxygen signatures produced through 1) biogeochemical mineralisation of sulphur to sulphate under oxidising conditions; 2) oxidation of continental biogenic emissions released into the atmosphere; 3) oxidation of marine DMS compounds; or 4) the release of primary seasalt aerosol (Figure 6). The only feasible mechanism of obtaining oxygen isotopes so enriched in ^{18}O would entail a degree of sulphate reduction. During initial stages of sulphate reduction, $\delta^{34}S\text{-}_{SO_4}$ and $\delta^{18}O\text{-}_{SO_4}$ signatures demonstrate a linear fractionation relationship, typical of a kinetic reaction mechanism. However at an advanced stage of sulphate reduction, equilibrium oxygen isotope exchange between reduced sulphur compounds and ambient water enables enrichment of ^{18}O in residual sulphur compounds dependent upon the temperature and isotopic composition of the surrounding water (enrichment ~ +28 ‰ at cave temperature of 10.4°C; cf. Fritz et al., 1989). Given that the average $\delta^{18}O\text{-}_{H_2O}$ composition of the drip water feeding stalagmite CC-Bil has a value of -5.4 ‰, equilibrium isotopic exchange during sulphate reduction would thus impart an oxygen isotopic composition approaching +23 ‰ in the residual sulphate, similar to that measured in stalagmite CC-Bil (Table

4). The offset between the lowest measured $\delta^{18}O\text{-}_{CAS}$ composition and the proposed equilibrium value of +23 ‰ may indicate a small contribution from the re-oxidation of sulphur compounds and the direct incorporation of an oxygen atom from water during sulphite oxidation. The range in $\delta^{18}O\text{-}_{CAS}$ signatures through time is thus likely explained through differences in the oxygen isotope exchange rates according to changes in the oxygen isotope composition of ambient water, temperature variations and the degree of re-oxidation (Brunner et al., 2005).

Given the extent of sulphate reduction inferred to occur along the drip water flow path, provenancing the source of additional sulphate using isotopic end member analysis is not possible. The following two mechanisms may produce drip waters at Crag Cave with sulphate isotopic compositions similar to those measured in CC-Bil. 1) The oxidation of pyrite to sulphate would typically contribute a source of isotopically light sulphur. Subsequent reduction of sulphate may produce residual sulphate enriched in ^{34}S and ^{18}O. Such a mechanism would have to occur under a system where regions of reduction are spatially isolated from areas of sulphide oxidation, thus allowing kinetic fractionation and enrichment of ^{34}S in the residual sulphate pool. Given the local presence of pyrite within bedrock horizons sampled from elsewhere within the cave (Tooth and Fairchild, 2003), this remains a potential source and cannot be disregarded conclusively. 2) Alternatively, the mineralisation of organic sulphur compounds to sulphate may contribute an additional source of sulphur with similar isotopic composition to that found in atmospheric precipitation. Extensive cyclical sulphate reduction/re-oxidation will enrich oxygen isotopes to a few per mille lighter than the equilibrium value of +23 ‰, whilst sulphur isotopes will undergo very little net fractionation between atmospheric deposition and drip

590 water composition as isotope mass balance is maintained. Net fractionation of sulphur
591 isotopes would be close to unity and reduction/oxidation would have to take place
592 without extensive product loss from the reactant pool. The sulphur isotopic
593 composition of speleothem CAS should thus reflect the isotopic composition of
594 atmospheric sulphur deposition, assuming minimal fractionation during uptake and
595 cycling through vegetation. The soil and vegetation thus acts as a store of organic
596 sulphur which is slowly released into dripwater flowpaths and speleothem calcite (cf.
597 Einsiedel et al., 2006).
598
599 Thus, based on $\delta^{34}S$ and $\delta^{18}O$ signatures obtained from speleothem CAS at Crag
600 Cave, the drip water feeding stalagmite CC-Bil appears to be subjected to reducing
601 conditions along the flowpath, mostly likely within the till. The water-saturated nature
602 of the fine grained, clay rich till above the cave provides the necessary conditions for
603 sulphate reduction, whilst patches of iron staining and soil pH as low as 3.5 may be
604 indicative of sulphide oxidation utilising FeIII as an oxidising agent under sub-oxic
605 conditions (Soil profile descriptions obtained from Tooth, 2000). For pyrite oxidation
606 and subsequent reduction to produce isotopic values similar to those observed in
607 speleothem CAS, processes of oxidation and reduction must be spatially separate.
608 Where cyclical sulphate reduction/re-oxidation is apparent, the re-oxidation of
609 reduced sulphur compounds draws the $\delta^{18}O$ composition of the residual sulphate away
610 from the equilibrium value and may be extensive enough to reverse the kinetic
611 isotopic enrichment of ^{34}S such that there is very little net fractionation of source
612 sulphur compounds.
613
614

615

616 **7. CONCLUSIONS**

617

618 There is currently very limited knowledge regarding the historical impacts of
619 increased SO_2 emissions from anthropogenic pollution at the local and regional scale.
620 Here, stalagmites have been demonstrated to contain sulphur in the form of calcite
621 associated sulphate which can be readily extracted and analysed for $\delta^{34}S\text{-}_{SO_4}$ and $\delta^{18}O\text{-}$
622 $_{SO_4}$ signatures. Using the techniques established above, sulphur and oxygen isotope
623 measurements are conducted using approximately 200 mg of calcite powder
624 (equivalent to just 35 μg of S) to obtain a time series record of sulphur inputs to the
625 karst system. Source partitioning of the constituent sulphate using end-member
626 isotopic analysis, sea salt ratios to chloride and bedrock ratios of Ca/SO_4, has
627 identified the dominant component of sulphur at Browns Folly Mine to be of
628 anthropogenic origin reflecting the industrial nature of the surrounding region.
629 Sulphur and oxygen isotope ratios of speleothem CAS at Crag Cave, W. Ireland,
630 reflect processes of sulphate reduction along drip water flow paths and are therefore
631 unsuitable for directly obtaining atmospheric sulphur records. Thus the potential for
632 speleothems to be used as archives of atmospheric sulphur pollution appears
633 encouraging where sediments overlying the cave system are oxidising throughout, as
634 might be expected where thin brown earth soils are found in many temperate and
635 Mediterranean climate zones. Where stalagmites are fed by drip waters of low redox
636 status, for example at high latitudes where clay rich tills or peat soils are frequently
637 found, their use as archives of atmospheric sulphur pollution appears limited due to
638 the extensive fractionation associated with processes of sulphate reduction. However,
639 use of sulphate sulphur and oxygen isotopes as indicators of reducing status may have

important implications in future speleothem studies for the interpretation of additional palaeoclimatic variables. At carefully selected cave sites, speleothems hold the potential to record short term variability in atmospheric sulphur loading and thereby enable an understanding of the local and regional significance of anthropogenic versus natural sulphur aerosols in forcing climatic change.

8. ACKNOWLEDGEMENTS

The authors would like to thank the UK Natural Environment Research Council (NERC) for funding this work (Grant NE/C511805/1). Thanks to Drs. K. Jarvis and K. Linge at the NERC ICP-MS facility, Kingston University for assistance with sulphur analysis. Dr. L. Baldini provided data for the average drip water oxygen isotopic composition at Crag cave and Dr. Dominique Genty supplied data for the average drip water oxygen isotopic composition at Browns Folly Mine. Dr. Rob Newton and two anonymous referees provided valuable comments and suggestions which helped improve this paper.

9. REFERENCES

663 Aherne, J and Farrell, E.P. (2002) Deposition of sulphur, nitrogen and acidity in
664 precipitation over Ireland: chemistry, spatial distribution and long-term trends.
665 *Atmospheric Environment*, **36**, 1379-1389.
666
667 Baker, A., Genty, D., Dreybodt, W., Barnes, W., Mockler, N and Grapes, J. (1998)
668 Testing theoretically predicted stalagmite growth rate with recently annually
669 laminated samples: Implications for past stalagmite deposition. *Geochimica et*
670 *Cosmochimica Acta*, **62**, 393-404.
671
672 Baker, A., Mockler, N., Barnes, W. (1999) Fluorescence intensity variations of
673 speleothem forming groundwaters: Implications for paleoclimate
674 reconstruction. *Water Resources Research*, **35**, 407-413.
675
676 Baldini, J.U.L, McDermott, F., Baker, A., Baldini, L.M., Mattey, D.P and Railsback.,
677 L.B. (2005) Biomass effects on stalagmite growth and isotope ratios: A 20^{th}
678 century analogue from Wiltshire, England. *Earth and Planetary Science*
679 *Letters*, **240**, 486-494.
680
681 Baldini, J.U.L., McDermott, F. and Fairchild, I.J. (2006) Spatial variability in cave
682 drip water hydrochemistry: Implications for stalagmite palaeoclimate records.
683 *Chemical Geology*, **235**, 390-404.
684
685 Barkan, E. and Luz, B. (2005) High precision measurements of $^{17}O/^{16}O$ and
686 $^{18}O/^{16}O$ ratios in H_2O. *Rapid communications in Mass Spectrometry*, **19**
687 (24), 3737-3742
688

689 Barker, A.P., Newton, R.J., Bottrell, S.H. and Tellam. J.H. (1998) Processes affecting
690 groundwater chemistry in a zone of saline intrusion into an urban sandstone
691 aquifer. *Applied Geochemistry*, **13**, 735-749.
692
693 Bottrell, S.H. and Novak, M. (1997) Sulphur isotopic study of two pristine sphagnum
694 bogs in the western British Isles. *The Journal of Ecology*, **85** (2) 125-132
695
696 Bottrell, S.H. and Coulson, J.P. (2003) Preservation of environmental sulphur isotope
697 records in maritime peats: a test of baseline pre-anthropogenic signal and
698 diagenetic effects in a mid-Pleistocene peat. *Chemical Geology*, **201**, 185-190.
699
700 Bottrell, S.H. and Newton, R.J. (2006) Reconstruction of changes in global sulphur
701 cycling from marine sulphate isotopes. *Earth-Science Reviews*, **75**, 59-83.
702
703 Bottrell, S.H. (2007) Stable isotopes in aqueous sulphate as tracers of natural and
704 contaminant sulphate sources: a reconnaissance study of the Xingwen karst
705 aquifer, Sichuan, China. In: Natural and Anthropogenic Hazards in Karst
706 Areas: Recognition, Analysis and Mitigation (eds. Parise, M and Gunn, J.).
707 *Geological Society, London, Special Publications*, **279**, 123-135
708
709 Brunner, B., Bernasconi, S.M., Kleikemper, J. and Schroth, M.H (2005) A model for
710 oxygen and sulfur isotope fractionation in sulfate during bacterial sulfate
711 reduction processes. *Geochimica et Cosmochimica Acta*, **69**, 4773 – 4785.
712

713 Calhoun, J., Bates, T and Charlson, R. (1991) Sulphur isotope measurements of
714 submicrometer sulphate aerosol particles over the Pacific Ocean. *Geophysical*
715 *Research Letters*, **18**, 1877 – 1880.
716
717 Coulson, J.P. Bottrell, S.H. and Lee, J.A. (2005) Recreating atmospheric sulphur
718 deposition histories from peat stratigraphy: Diagenetic conditions required for
719 signal preservation and reconstruction of past sulphur deposition in the
720 Derbyshire Peak District, UK. *Chemical Geology*, **218**, 223-248
721
722 Einsiel, F and Mayer, B. 2005. Sources and processes affecting sulphate in a karstic
723 groundwater system of the Franconian Alb, Southern Germany.
724 *Environmental Science and Technology*, **39**, 7118-7125
725
726 Fairchild, I.J., Smith, C.L., Baker, A., Fuller, L., Spötl, C., Mattey, D., McDermott, F
727 and E.I.M.F. (2006a) Modification and preservation of environmental signals
728 in speleothems. *Earth-Science Reviews*, **75**, 105-153
729
730 Fairchild, I.J., Tuckwell, G.W., Baker, A and Tooth, A.F. (2006b) Modelling of drip
731 water hydrology and hydrogeochemistry in a weakly karstified aquifer (Bath,
732 UK): Implications for climate change studies. *Journal of Hydrology*, **321**, 213-
733 231
734
735 Fitzgerald, J.W. (1976) Sulphate ester formation and hydrolysis: a potentially
736 important yet often ignored aspect of the sulphur cycle of aerobic soils.
737 *Bacteriological Reviews*, **40**, 698-721.

738

739 Frisia, S., Borsato, A., Fairchild, I.J. and Susini, J. (2005) Variations in atmospheric
740 sulphate recorded in stalagmites by synchrotron micro-XRF and XANES
741 analyses. *Earth and Planetary Science Letters*, **235**, 729-740

742

743 Fritz, P., Basharmal, G.M., Drimmie, R.J., Ibsen, J., and Qureshi, R.M. (1989)
744 Oxygen isotope exchange between sulphate and water during bacterial
745 reduction of sulphate. *Chemical Geology (Isotope Geoscience Section)* **79**, 99-
746 105.

747

748 Fry, B., Silva, S.R., Kendall, C., Anderson, R.K. (2002) Oxygen isotope corrections
749 for online $\delta^{34}S$ analysis. *Rapid Communications in Mass Spectrometry*, **16**,
750 854-858.

751

752 Gellatly, A.M. and Lyons, T.W. (2005) Trace sulphates in mid-Proterozoic carbonates
753 and the sulphur isotope record of biospheric evolution. *Geochimica et*
754 *Cosmochimica Acta*, **69**, 3813-3829.

755

756 Holland, H.D. (1978) *The chemistry of the atmosphere and oceans*. Wiley, New York.

757

758 Holt, B.D., Cunningham, P.T and Kumar, R. (1981) Oxygen isotopy of atmospheric
759 sulphates. *Environmental Science and Technology*, **15**, 804 – 808.

760

761 Holt, B.D., Kumar, R. and Cunningham, P.T. (1982) Primary sulphates in
762 atmospheric sulphates: Estimation in oxygen isotope ratio measurements.
763 *Science*, **217**, 51-53.
764
765 Holt, B.D and Kumar, R. (1991) Oxygen isotope fractionation for understanding the
766 sulphur cycle. In: Stable isotopes: natural and anthropogenic sulphur in the
767 environment. SCOPE 43 (eds. H.R. Krouse and V.A. Grinenko). Wiley, New
768 York. Pp. 27-41.
769
770 Hurtgen, M.T., Arthur, M.A., Suits, N.S. and Kaufman, A.J. 2002.The sulphur
771 isotopic composition of Neoproterozoic seawater sulfate: implications for a
772 snowball Earth? *Earth and Planetary Science Letters*, **203**, 413-429
773
774 IAEA., 2004. Reference materials catalogue 2004-2005, Analytical Quality Control
775 Services, International Atomic Energy Agency, Vienna
776
777 Isaksson, E., Kekonen, T., Moore, J and Mulvaney, R. (2005) The methanesulfonic
778 acid (MSA) record in a Svalbard ice core. *Annals of Glaciology*, **42**, 345-351.
779
780 Jamieson, R.E. and Wadleigh, M. A. (1999) A study of the oxygen isotopic
781 composition of precipitation sulphate in Eastern Newfoundland. *Water, Air*
782 *and Soil Pollution*, **110**, 405-420.
783

784 Jenkins, K.A. and Bao, H. (2006) Multiple oxygen and sulphur isotope compositions
785 of atmospheric sulphate in Baton Rouge, LA, USA. *Atmospheric*
786 *Environment*, **40**, 4528-4537
787
788 Jordan, C. (1997) Mapping of rainfall chemistry in Ireland 1972-94. *Biology and*
789 *Environment: Proceedings of the Royal Irish Academy*, **97B** (1), 53-73.
790
791 Kawamura, H., Matsuoka, N., Momoshima, N., Koike, M and Takashima, Y. (2006)
792 Isotopic evidence in tree rings for historical changes in atmospheric sulphur
793 sources. *Environmental Science and Technology*, **40**, 5750 – 5754.
794
795 Krouse, R.H. and Mayer, B. (1999) Sulphur and oxygen isotopes in sulphate. In:
796 Environmental tracers in subsurface hydrology. (eds.Cook, P.G. and Herczeg,
797 A.L) Kluwer academic publishers. Pp. 195 – 231.
798
799 Lefohn, A.S., Husar, J.D. and Rudolf, H.B. (1999) Estimating historical
800 anthropogenic global sulphur emission patterns for the period 1850-1990.
801 *Atmospheric Environment*, **33**, 3435-3444.
802
803 Likens, G.E., Driscoll, C.T., Buso, D.C., Mitchell, M.J., Lovett, G.M., Bailley, S.W.,
804 Saiccama, T.G., Reiners, W.A. and Alewell, C. (2002) The biogeochemistry
805 of sulphur at Hubbard Brook. *Biogeochemistry*, **60**, 235-316.
806
807 Lloyd, R.M. (1967) Oxygen-18 composition of oceanic sulphate. *Science*, **156**, 1228-
808 1231

Lloyd, R.M. (1968) Oxygen isotope behaviour in the sulphate-water system. *Journal of Geophysical Research*, **73**, 6099-6110.

Mayer, B., Fritz, P., Kneif, K., Li, G., Fischer, M., Rehfuess, K.E. and Krouse, H.R. (1992) Evaluating pathways of sulphate between the atmosphere and hydrosphere using stable sulphur and oxygen isotope data. In: *Isotope Techniques in Water Resources. Proceedings of an international conference in Vienna, Austria.* Pp3-17. IAEA, Vienna, Austria, March 11-15, 1991.

Mayer, B., Fritz, P., Prietzel, J. and Krouse, H.R. (1995a) The use of stable sulphur and oxygen isotope ratios for interpreting the mobility of sulphate in aerobic forest soils. *Applied Geochemistry*, **10**, 161-173.

Mayer, B., Feger, K.H., Geisemann, A and Jäger, H. (1995b) Interpretation of sulphur cycling in two catchments in the Black Forest (Germany) using stable sulphur and oxygen isotope data. *Biogeochemistry*, **30,** 31-58.

Mayer, B. (1998) Potential and limitations of using sulphur isotope abundance ratios as an indicator for natural and anthropogenic induced environmental change. In: *Isotope techniques in the study of environmental change. Proceedings of an international conference in Vienna, Austria*. Pp 423-435. IAEA, Vienna Austria, 14-18th April 1997.

Mayer, B., Alpay, S., Gould, W.D., Lortie, L. and Rosa, F. (2007) The onset of anthropogenic activity recorded in lake sediments in the vicinity of the Horne smelter in Quebec, Canada: Sulphur isotope evidence. *Applied Geochemistry*, **22**, 397-414.

McDermott, F., Frisia, S., Huang, Y., Longinelli, A., Spiro, B., Heaton, T.H.E., Hawkesworth, C.J., Borsato, A., Keppens, E., Fairchild, I.J., van der Borg, K., Verheyden, S. and Selmo, E. (1999) Holocene climate variability in Europe: Evidence from $\delta^{18}O$, textural and extension-rate variations in three speleothems. *Quaternary Science Reviews*, **18**, 1021-1038.

Newton, R.J., Pevitt, E.L., Wignall, P.B. and Bottrell, S.H. 2004. Large shifts in the isotopic composition of seawater sulphate across the Permo-Triassic boundary in northern Italy. *Earth and Planetary Science Letters*, **218**, 331-345

Nielson, H. (1974) Isotopic composition of the major contributors to atmospheric sulphur. *Tellus*, **XXVI**, 211-221.

Novák, M., Vile, M.A., Bottrell, S.H., Štěpánová, M., Jačková, I., Buzek, F., Přechova, E. and Newton, R. (2005) Isotope sytematics of sulphate-oxygen and sulphate-sulphur in six European peatlands. *Biogeochemistry*, **76**, 187-213.

Patris, N., Delmas, R.J, and Jouzel, J. (2000) Isotopic signatures of sulphur in shallow Antarctic ice cores. *Journal of Geophysical Research*, **105(D6)**, 7071-7078.

Patris, N., Delmas, R.J., Legrand, M., Angelis, M. De., Ferron, F.A., Stievenard, M and Jouzel, J. (2002) First sulphur isotope measurements in central Greenland ice cores along the preindustrial and industrial periods. *Journal of Geophysical Research*, **107, D11 4115,** ACH 6-1 - ACH 6-11.

Pingitore, N., Meitzner, G and Love, K. (1995) Identification of sulphate in natural carbonates by X-ray absorption spectroscopy. *Geochimica et Cosmochimica Acta,* **59,** 2477-2483.

Rees, C.E., Jenkins, W.J. and Monster, J. (1978) The sulphur isotopic composition of ocean water sulphate. *Geochimica et Cosmochimica Acta,* **42** (4), 377-381

Rozanski, K., Araguás- Araguás, L and Gonfiantini, R. (1993) Isotopic patterns in modern global precipitation. In *Climate Change in Continental Isotopic Records, Geophysical Monograph Series*, **78,** (eds. P.K. Swart, et al.). pp. 1-36, AGU, Washington, DC, 1993.

Smart, P.L. and Friederich, H. (1986) Water movement and storage in the unsaturated zone of a maturely karstified carbonate aquifer, Mendip Hills, England. Proceedings of the Conference on Environmental Problems in Karst Terrains and their Solutions. National Water Wells Association, Bowling Green, KY, pp57-87, October 28-30 1986.

Smith, R.J., Pitcher, H and Wigley, T.M.L. (2001) Global and regional anthropogenic sulphur dioxide emissions. *Global and Planetary Change*, **29**, 99-119.

Taylor, B.E., Wheeler, M.C and Nordstrom, D.K. (1984) Stable isotope geochemistry of acid mine drainage: Experimental oxidation of pyrite. *Geochimica et Cosmochimica Acta*, **48**, 2669 – 2678.

Tooth, A.F. (2000) Controls on the geochemistry of speleothem-forming karstic drip waters. Ph.D thesis, University of Keele.

Tooth, A.F. and Fairchild, I.J. (2003) Soil and karst aquifer hydrological controls on the geochemical evolution of speleothem forming drip waters, Crag Cave, southwest Ireland. *Journal of Hydrology*, **273**, 51-68.

Toran, L. and Harris, R.F. (1989) Interpretation of sulphur and oxygen isotopes in biological and abiological sulfide oxidation. *Geochimica et Cosmochimica Acta*, **53**, 2341 – 2348.

Wadleigh, M.A., Schwarcz, H.P. and Kramer, J.R. (1996) Isotopic evidence for the origin of sulphate in coastal rain. *Tellu*s, **48B**, 44-59.

Wortmann, U.G., Chernyavsky, B.C., Bernasconi, S.M., Brunner, B., Böttcher, M.E. and Swart, P.K (2007) Oxygen isotope biogeochemistry of pore water sulphate in the deep biosphere: Dominance of isotope exchange reactions with ambient

water during microbial sulphate reduction (ODP Site 1130). *Geochimica et Cosmochimica Acta*, **doi:10.1016/j.gca.2007.06.033**

Zhao, F.J., Spiro, B., Poulton, P.R and McGrath, S.P. (1998) Use of sulphur isotope ratios to determine anthropogenic sulphur in a grassland ecosystem. *Environmental Science and Technology*, **32**, 2288-2291.

948 **Table 1:** Sulphur concentration and isotope ratios in stalagmite BFM-Boss
949

Distance below top of stalagmite (mm)	Year of deposition	S (ppm)	$\delta^{34}S\text{-}SO_4$ Vs CDT (Rep 1)	$\delta^{34}S\text{-}SO_4$ Vs CDT (Rep 2)	$\delta^{34}S\text{-}SO_4$ Vs CDT (Average)	Standard deviation between replicates	$\delta^{18}O\text{-}SO_4$ Vs V-SMOW (‰)
0-4	1995 - 1990	264	3.6	4.0	3.8	0.24	10.6
4-8	1990 - 1984	214	3.5	3.5	3.5	0.02	10.5
8-12	1984 - 1973	160	3.8	3.3	3.5	0.35	10.3
12-16	1973 - 1958	239	3.7	3.3	3.5	0.22	10.9
16-20	1958 - 1938	130	-----	4.3	4.3	-----	13.6
20-24	1938 - 1916	169	-----	5.5	5.5	-----	13.7

950
951
952
953
954
955 **Table 2:** Bedrock sulphur concentrations and isotope ratios
956

Rock	S concentration (ppm)	Ca/SO_4 ratio (weight ratio)	$\delta^{34}S\text{-}SO_4$ Vs CDT
Browns Folly Mine 1	166	806	22.0
Browns Folly Mine 2	212	631	22.0
Browns Folly Mine 3	269	497	17.6
Browns Folly Mine 5	241	555	18.9
Browns Folly Mine 6	191	700	21.3
Browns Folly Mine 7	156	858	20.1
Browns Folly Mine 10	312	429	17.9
Crag Cave 1	52	2573	n.d
Crag Cave 2	51	2623	n.d
Crag Cave 3	92	1454	n.d

957
958
959
960 **Table 4:** Sulphur concentration and isotope ratios in stalagmite CC-Bil
961

Distance below top of stalagmite (mm)	S concentration (ppm)	$\delta^{34}S\text{-}SO_4$ Vs CDT (‰)	$\delta^{18}O\text{-}SO_4$ Vs V-SMOW (‰)
0-10	142	18.6	23.9
10-20	173	17.6	23.0
20-30	184	17.5	22.7
30-40	107	16.9	20.7
40-50	134	16.8	22.5
50-60	184	18.5	22.8
60-70	178	17.7	19.2
70-80	n.d	19.1	22.6
80-90	n.d	19.1	22.5
90-100	n.d	18.7	22.7

Table 3: Drip site ion chemistry

Cave Site	Drip site	n^* =	Ca^{2+} (mg/l)	SO_4^{2-} (mg/l)	Cl^- (mg/l)	Ca/SO_4 ratio	% SSS	% sulphur from bedrock CAS in drip waters
Browns Folly Mine, UK Midlands (January 1996 – February 1998)	BFM-Boss	14	99.0 (14.5)	11.0 (3.4)	24.2 (16.2)	9.0 (3.9)	28.7 (15.0)	1.4
Crag Cave, S.W Ireland. Lower chamber. 2006	CC-Bil Seepage flow	1	182.8	7.9	19.8	23.1	35.1	1.1
Crag Cave, S.W Ireland. Lower chamber. August 1997	R Seepage flow	8	113.7 (4.7)	8.2 (0.1)	21.6 (0.2)	13.8 (0.5)	36.7 (0.3)	0.7
Crag Cave, S.W Ireland. Lower chamber. August 1997	X Seepage flow	10	137.1 (33.2)	8.1 (0.1)	20.8 (0.3)	17.0 (4.4)	36.2 (0.6)	0.8
Crag Cave, S.W Ireland. Lower chamber. August 1997	Z Seepage flow	11	133.3 (31.7)	8.4 (0.05)	21.7 (0.1)	15.8 (3.8)	36.0 (0.2)	0.8

Data from Crag Cave drip sites A-Z obtained from Tooth, 2000

$^*n$ represents the number of field samples. 1 standard deviation (1 SD) is given in parentheses.

Figure 1: Sources and cycling of sulphur contributing to bulk stalagmite sulphate composition with characteristic $\delta^{34}S$ compositions. Values are given for predominantly anthropogenic sulphate in rain in industrialised countries of the northern hemisphere (range -3 to +9 ‰; Mayer, 1998); sulphate aerosol from ocean surface (+21 ‰; Rees, 1978); marine biogenic emissions as DMS (+15.6 +/- 3.1 ‰; Calhoun et al., 1991); continental and intertidal biogenic emissions (0 to -30 ‰; Nielson, 1974); volcanic eruptions (~ 0 ‰; Nielson, 1974).

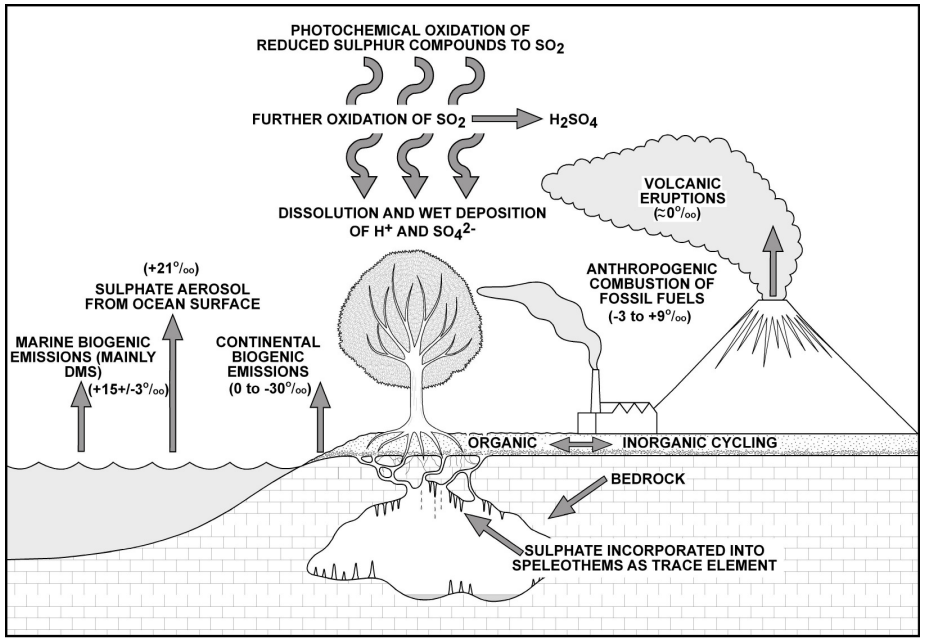

Figure 2: Diagram showing the two approaches (centrifugation and filtration) to extracting and concentrating sulphate from speleothem calcite as barium sulphate prior to $\delta^{34}S$ and $\delta^{18}O$ analysis.

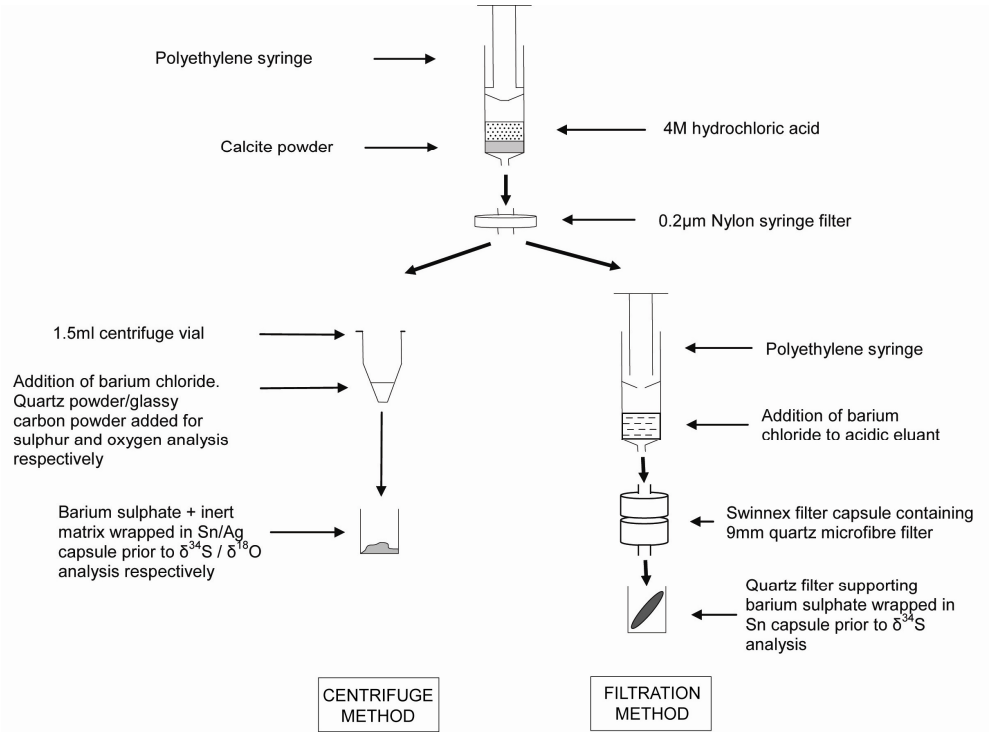

Figure 3: Sulphur concentration, $\delta^{34}S\text{-}_{CAS}$ and $\delta^{18}O\text{-}_{CAS}$ in stalagmite BFM-Boss.

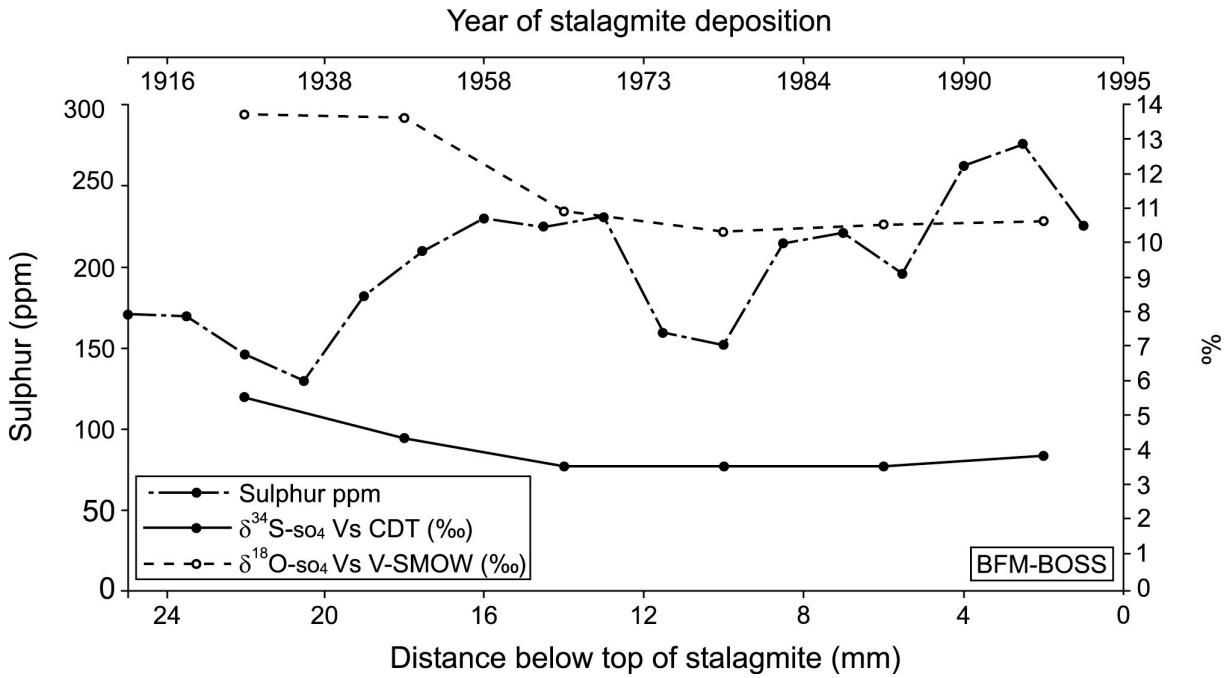

Figure 4: Suphur concentration, $\delta^{34}S\text{-}_{CAS}$ and $\delta^{18}O\text{-}_{CAS}$ in stalagmite CC-Bil.

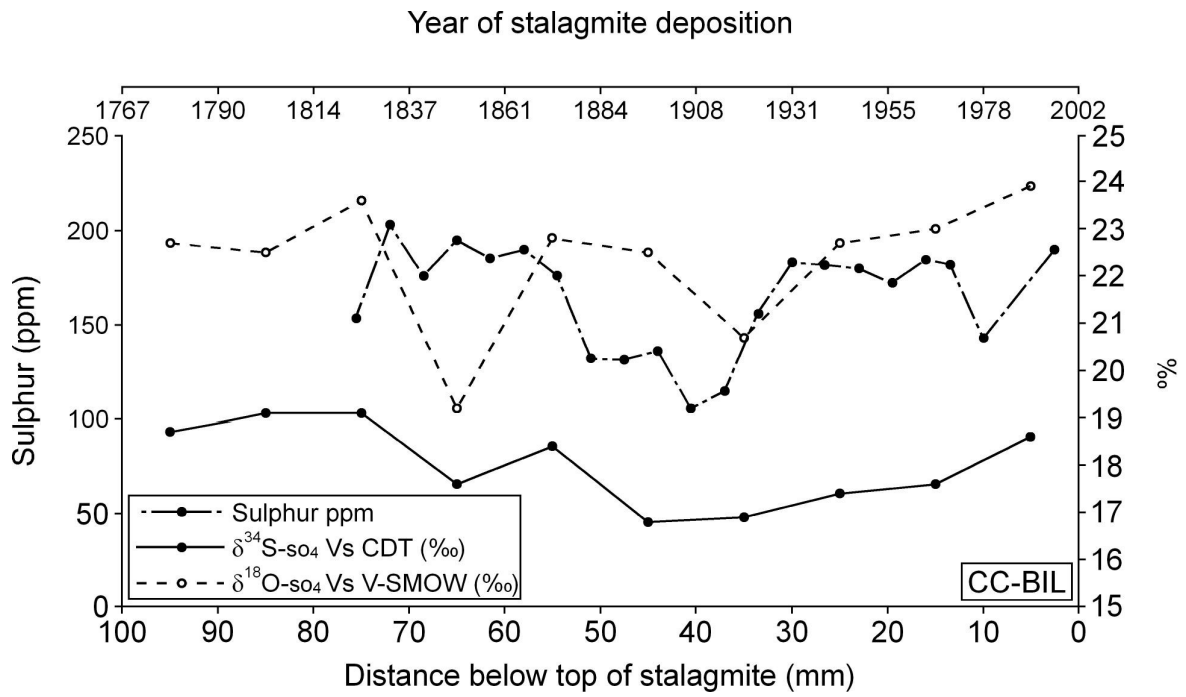

Figure 5: Diagram illustrating the range of $\delta^{34}S\text{-}_{CAS}$ and $\delta^{18}O\text{-}_{CAS}$ in stalagmite BFM-Boss compared to potential sulphate sources. The measured range of $\delta^{18}O$ in BFM-Boss is encompassed within the region of precipitation sulphate. Range of measured $\delta^{34}S\text{-}SO_4$ in precipitation for industrialised countries of the northern hemisphere obtained from Mayer et al., 1998. Range of published $\delta^{18}O\text{-}SO_4$ in precipitation for mid-latitude sites obtained from Jenkins and Bao, 2006; Jamieson and Wadleigh, 1999.

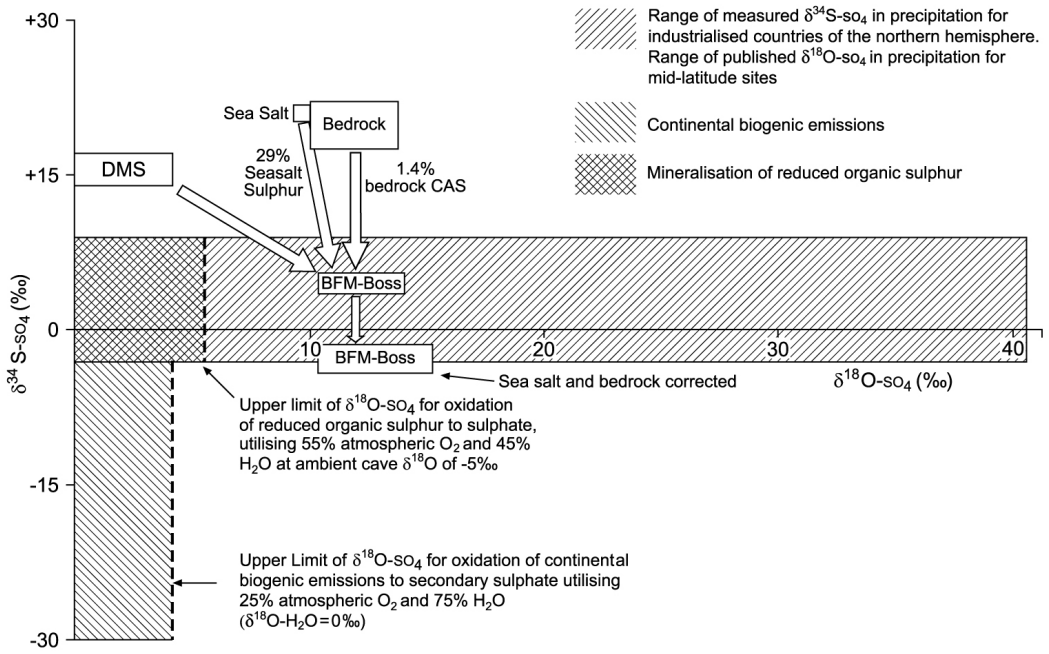

Figure 6: Diagram illustrating the range of $\delta^{34}S\text{-}_{CAS}$ and $\delta^{18}O\text{-}_{CAS}$ in stalagmite CC-Bil compared to potential sulphate sources. The range of measured $\delta^{34}S\text{-}_{CAS}$ and $\delta^{18}O\text{-}_{CAS}$ is distinct compared to other sources of sulphate, suggesting additional sulphur cycling must modify the composition of the source materials prior to incorporation into stalagmite calcite. Range of measured $\delta^{34}S\text{-}_{SO_4}$ in precipitation for industrialised countries of the northern hemisphere obtained from Mayer et al., 1998. Range of published $\delta^{18}O\text{-}_{SO_4}$ in precipitation for mid-latitude sites obtained from Jamieson and Wadleigh, 1999; Jenkins and Bao, 2006.